

COMPUTATIONAL FLUID DYNAMICS ANALYSIS IN SUPPORT  
OF THE SIMPLEX TURBOPUMP DESIGN

N95-70873

Roberto Garcia, Lisa W. Griffin, Theodore G. Benjamin  
Joni W. Cornelison, Joseph H. Ruf, and Robert W. Williams  
Computational Fluid Dynamics Branch  
NASA/Marshall Space Flight Center  
Marshall Space Flight Center, AL 35812

## OVERVIEW:

Simplex is a turbopump that is being developed at NASA/Marshall Space Flight Center (MSFC) by an in-house team. The turbopump consists of a single-stage centrifugal impeller, vaned-diffuser pump powered by a single-stage, axial, supersonic, partial admission turbine. The turbine is driven by warm gaseous oxygen tapped off of the hybrid motor to which it will be coupled. Rolling element bearings are cooled by the pumping fluid. Details of the configuration and operating conditions are given by Marsh [1]. CFD has been used extensively to verify one-dimensional (1D) predictions, assess aerodynamic and hydrodynamic designs, and to provide flow environments. The complete primary flow path of the pump-end and the hot gas path of the turbine, excluding the inlet torus, have been analyzed. All CFD analyses conducted for the Simplex turbopump employed the pressure based Finite Difference Navier-Stokes (FDNS) code using a standard k- $\epsilon$  turbulence model with wall functions. More detailed results are presented by Garcia et. al. [2]. To support the team, loading and temperature results for the turbine rotor were provided as inputs to structural and thermal analyses, and blade loadings from the inducer were provided for structural analyses.

## DISCUSSION:

The hot gas path of the Simplex turbine consists of an inlet torus, a ring of twelve converging-diverging nozzles, a wheel of 95 impulse rotors, and a 7.6 inch diameter exhaust pipe. Six of the nozzles are blocked in a pattern of one active arc of admission and one inactive arc so it operates at 45% admission. The total pressure at the inlet of the nozzle is 800 psi, and the total-to-static pressure ratio is 15. The impulse turbine pressure drop is taken across the nozzle. The inlet total temperature is 800° R. The total mass flow rate is 1.54 lbm/sec per nozzle. The wheel speed is 25,000 rpm, and the turbine is to supply 700 hp. The velocity ratio of the rotor is 0.355.

The nozzle analysis is fully three-dimensional (3D). The inlet to throat area ratio is 2.42, and the exit to throat area ratio is 2.78. A total pressure of 800 psi was held constant at the inlet and a static pressure of 53.3 psi was held constant at the exit. The walls of the nozzle were assumed to be "no-slip" and adiabatic and to have a zero normal pressure gradient. The results show the nozzle is overexpanded. The pressure at the exit of the diverging section is approximately

40 psi and then increases to the back pressure across an oblique shock. Some attempts were made to resize the nozzle to ensure isentropic flow, but size constraints limited modifying the nozzle design. Pressure at the exit of the nozzle varies from 35 psi to 75 psi. The mach number reaches 3.5 at the exit of the divergent section and shocks down to 2.5 at the exit to the nozzle ring. The variation in the velocity at the exit is acceptable.

The rotor analysis included design parametrics. The Simplex rotor blades are straight in the radial direction, so even though tip leakage would produce some 3D effects, calculations could be performed two dimensionally (2D) at the midspan. The inlet boundary was at the nozzle exit. Flow conditions obtained from the 1D nozzle flow analysis were imposed. A static pressure of 53.3 psi was imposed at the exit. Results are shown in figure 1. There is a separation on the suction surface of the blade. The calculated power output per full flowing rotor is 31.7 hp. Six

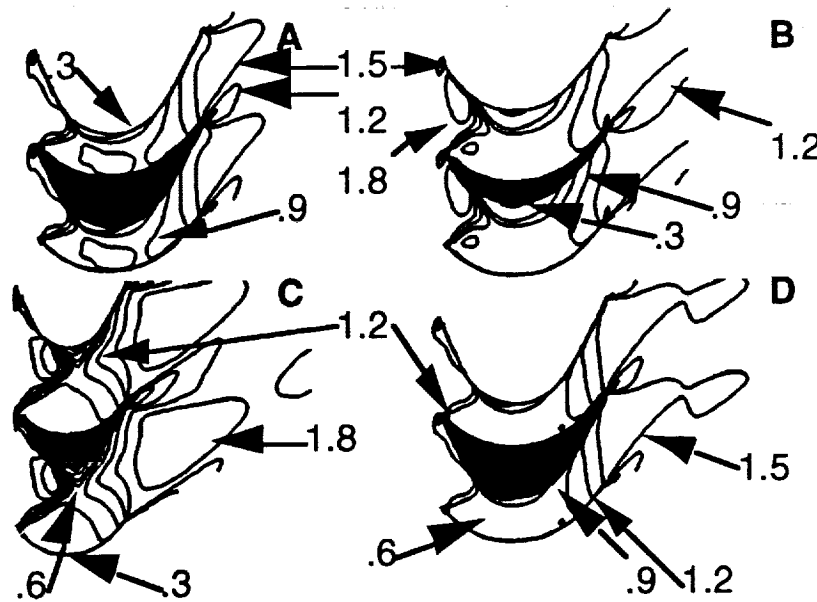


Figure 1. Two-dimensional rotor parametrics, showing mach number contours

alternate blade designs did not improve the flow field. After this, a 3D shrouded rotor was analyzed. Losses of 12% for partial admission and 5% for tip leakage were assumed based on the literature. The flow field improved relative to the 2D rotor by producing a smaller separated region and a slight increase to 950 hp, which is sufficient.

The objectives of the disk cavity analysis were to determine the effect of the bearing coolant leakage on axial thrust and on turbine performance. The initial bearing coolant circuit consisted of 4.5 lbm/sec of liquid oxygen (LOX) being diverted from the impeller discharge to cool the bearings. Of this coolant flow, 2.7 lbm/sec was returned to the impeller inlet and 1.8 lbm/sec leaked into the turbine disk cavity. The maximum transient load to which the bearings can

respond is 4,400 lbf. It was assumed that for a worst case the fluid would remain a liquid throughout the entire cavity. The cavity was modeled from the seal exit to the hot gas path. The flow field was assumed to be axisymmetric. The change in pressure from seal exit to hot gas path was calculated to be 1,100 psi, and the increase was basically linear with radius. The resultant axial force on the disk was 15,000 lbf. The performance loss due to coolant leakage into the hot gas path was estimated to be 15 points in turbine efficiency. Clearly, the axial load and performance detriment with the initial coolant circuit were unacceptable. The bearing coolant circuit was redesigned with 3.5 lbm/sec returning externally to the inducer inlet and 1.5 lbm/sec vented overboard. A small amount of gas from the turbine primary flow path is drawn into the cavity, across the straight seal, and out the overboard drain. For this case, the fluid in the cavity was assumed to be entirely a gas. Because this assumption necessitated imposing pressures at inlet and exit boundaries where pressures were known, the modeled domain included the disk cavity, rotor, and exhaust pipe. It was modeled as a 3D, periodic wedge that included one rotor passage. A pressure of 40 psi was assumed at the cavity/seal interface based on estimates from a forced vortex calculation. The rotor flow field is similar to that of the stand alone model. The pressure rise from seal to platform is approximately 30 psi. The pressure rise on the back side of the disk from centerline to platform is approximately 20 psi. The resultant force on the disk of 300 lbf is manageable. Flow of approximately 0.001 lbm/sec was calculated to be pulled from the hot gas path and into the cavity.

The pump flow path of the Simplex turbopump consists of an axial inlet, a three-bladed inducer, a six-bladed impeller, an eight-vaned diffuser, and a single-discharge volute. The minimum inlet LOX pressure is 45 psi at 164°R flowing at 89.8 lbm/sec, yielding a required suction specific speed ( $N_{ss}$ ) of approximately 25,000 at the design point speed. The discharge pressure required is 1,500 psi, 85% of which is generated by the radial impeller. Steady-state analyses were performed on each of the subcomponents that comprise the pump main flow path.

As a result of axisymmetric analyses of the pump inlet the inducer retaining nut was simplified from a parabolic curve shape to a shape made up of three flat surfaces. The inducer inlet relative flow angle is very similar for both geometries. Subsequent analyses were performed to arrive at an acceptable bearing coolant reentry scheme. The aforementioned bearing cooling circuit redesign necessitated routing the bearing coolant discharge back to the pump inlet outer diameter. Design iterations resulted in a design incorporating 10 reentry holes two inches upstream of the inducer. This configuration produced very little disturbance to the incoming flow.

The inducer analyses used the hub-to-shroud velocity distributions obtained from the inlet analysis. All cases assumed non-cavitated conditions. Grid sensitivity studies showed that while details of the flow field were affected by grid density, the overall performance and flow features were captured by coarse grids. The original inducer had a tip solidity of 2.68, but generated very

little head over the last third of the blade chord due to the small amount of diffusion through the inducer, producing losses nearly as large as the work input in the latter portion of the blade. The chord was reduced by one-third to improve the efficiency of the inducer, which coincided with rotordynamic needs to reduce the rotating mass outboard of the pump-end bearing. The resulting design produces a non-cavitated total pressure rise of 197 psi with a net hydraulic efficiency of 73%. The inducer flow field exhibited the typical secondary flow patterns present in these high-solidity rotating channels. Figure 2 shows an x-r projection of the flow through the inducer. The typical region of backflow is present at the inducer inlet near the blade tip. The inlet region of recirculation extends completely across the channel. Radially inward flow near the pressure surface tip was caused by the low momentum fluid (in the absolute reference frame) near the stationary shroud. This phenomenon was magnified by the model's zero tip clearance. The circumferentially averaged hub-to-shroud velocity profile was also obtained from these results.

The Simplex impeller incorporates six full-length blades with no partial blades and generates a total pressure rise of 1,300 psi. All but one of the cases were performed used the circumferentially averaged hub-to-shroud inducer-exit velocity profile as the inlet velocity condition. One case was run that included the actual inducer-exit velocity field (no averaging) and two impeller channels. The blade loading on adjacent blades was nearly identical, indicating that the clocking was acceptable. The baseline impeller design was determined to be acceptable. Typical of a centrifugal impeller, the hydraulic efficiency for the Simplex impeller was predicted to be high (95.6%). Analyses performed at off-design conditions showed that the impeller is insensitive to small variations in the incoming flow angle. The inlet relative flow angle was varied from  $13^\circ$  to  $23^\circ$  ( $18^\circ$  being the design point average angle) and the head coefficient varied from +10% to -7.5%, respectively, about the design point. The discharge absolute flow angle was nearly invariant over this range of inlet angle, which simplifies the design and analysis of the diffuser. Figure 3 shows the circumferentially averaged impeller exit hub-to-shroud flow distribution.

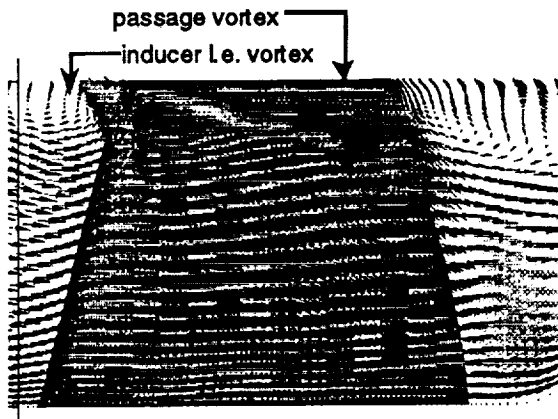


Figure 2. Inducer velocity vectors near the pressure surface, axial-radial projection

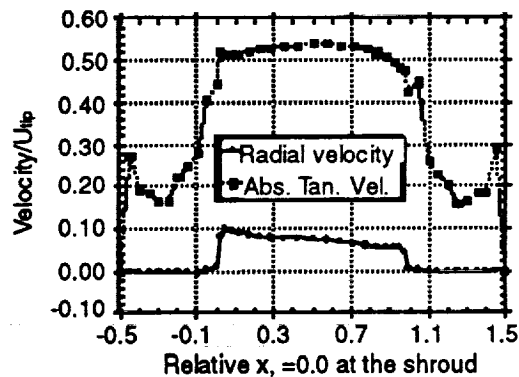


Figure 3. Impeller exit hub-to-shroud circumferentially averaged velocity profile

The initial CFD evaluation of the diffuser was performed on a 2D plane modeling a single diffuser channel. Results showed that at the impeller discharge flow angle of approximately  $10^\circ$ , some separation on the pressure surface of the vane would reduce performance. Since the impeller discharge angle was  $11.8^\circ$ , the diffuser performance was not acceptable. This necessitated a 3D model of the eight diffuser channels and volute, which allowed the inclusion of the hub-to-shroud velocity profile obtained from the impeller. The separation seen at the higher inlet flow angles cases studied in the 2D model worsened in the 3D results. The separation did not encompass the entire span of the vane but is limited to the span locations where the inlet flow angle was largest. The static pressure increase ( $\Delta P$ ) from the impeller exit to the diffuser exit was 118 psi. Therefore, parametrics were performed on a 3D  $45^\circ$  single-passage segment of the diffuser beginning at the impeller exit and proceeding through the diffuser exit. An exit region of constant circumferential cross-sectional area was appended downstream of the diffuser. A comparison between the full-geometry baseline design and the single-passage baseline validated this approach. Several design changes compatible with schedule and fabrication requirements were evaluated. The solution entailed a cutback on the leading edge of the vanes, which increased the flow angles at the entrance to the vanes and eliminated the blockage of flow by adjacent blades, yielding a  $\Delta P$  of 288 psi.

#### REFERENCES:

1. Marsh, M., "Simplex Turbopump Design," to be printed in the Proceedings of the 1994 Conference on Advanced Earth-to-Orbit Propulsion Technology, (R. J. Richmond and S. T. Wu eds) May 17-19, 1994 Marshall Space Flight Center, AL.
2. Garcia, R., Griffin, L. W., Benjamin, T. G., Cornelison, J. W., Ruf, J. H., Williams, R. W., "Computational Fluid Dynamics Analysis in Support of the Simplex Turbopump Design," to be printed in the Proceedings of the 1994 Conference on Advanced Earth-to-Orbit Propulsion Technology, (R. J. Richmond and S. T. Wu eds) May 17-19, 1994 Marshall Space Flight Center, AL.